Hum Genet
DOI 10.1007/s00439-010-0918-0

ORIGINAL INVESTIGATION

Transcriptome profile reveals AMPA receptor dysfunction in the hippocampus of the *Rsk2*-knockout mice, an animal model of Coffin–Lowry syndrome

Tahir Mehmood · Anne Schneider · Jérémie Sibillec · Patricia Marques Pereira · Solange Pannetier · Mohamed Raafet Ammar · Doulaye Dembele · Christelle Thibault-Carpentier · Nathalie Rouach · André Hanauer

Received: 1 September 2010 / Accepted: 5 November 2010

Abstract Coffin–Lowry syndrome (CLS) is a syndromic form of mental retardation caused by loss of function mutations in the X-linked *RPS6KA3* gene, which encodes RSK2, a serine/threonine kinase acting in the MAPK/ERK pathway. The mouse invalidated for the *Rps6ka3* (*Rsk2*-KO) gene displays learning and long-term spatial memory deficits. In the current study, we compared hippocampal gene expression profiles from *Rsk2*-KO and normal littermate mice to identify changes in molecular pathways. Differential expression was observed for 100 genes encoding proteins acting in various biological pathways, including cell growth and proliferation, cell death and higher brain function. The twofold up-regulated gene (*Gria2*) was of particular interest because it encodes the subunit GLUR2 of the AMPA glutamate receptor. AMPA receptors mediate most fast excitatory synaptic transmission in the central nervous system. We provide evidence that in the hippocampus of *Rsk2*-KO mice, expression of GLUR2 at the mRNA and at the protein levels is significantly increased, whereas basal AMPA receptor-mediated transmission in the hippocampus of *Rsk2*-KO mice is significantly decreased. This is the first time that such deregulations have been demonstrated in the mouse model of the Coffin–Lowry syndrome. Our findings suggest that a defect in AMPA neurotransmission and plasticity contribute to mental retardation in CLS patients.

T. Mehmood and A. Schneider contributed equally to this work.

Electronic supplementary material The online version of this article (doi:10.1007/s00439-010-0918-0) contains supplementary material, which is available to authorized users.

T. Mehmood · A. Schneider · P. Marques Pereira · S. Pannetier · M. R. Ammar · A. Hanauer (✉)
Department of Translational Medicine and Neurogenetics, Institut de Génétique et de Biologie Moléculaire et Cellulaire (IGBMC), Institut National de Santé et de Recherche Médicale (INSERM) U964/Centre National de Recherche Scientifique (CNRS) UMR 7104/Université de Strasbourg, 67404 Illkirch, France
e-mail: Andre.HANAUER@igbmc.fr

T. Mehmood
Department of Chemistry, University of Sargodha, Sargodha 40100, Pakistan

D. Dembele · C. Thibault-Carpentier
Microarray and Sequencing Platform, Institut de Génétique et de Biologie Moléculaire et Cellulaire (IGBMC), Institut National de Santé et de Recherche Médicale (INSERM) U964/Centre National de Recherche Scientifique (CNRS) UMR 7104/Université de Strasbourg, 67404 Illkirch, France

J. Sibillec · N. Rouach
Collège de France, 75005 Paris, France

Introduction

Coffin–Lowry syndrome (CLS; MIM#303600) is a rare syndromic form of mental retardation that is characterized by moderate to severe psychomotor retardation, growth retardation, facial and digital dysmorphisms, as well as progressive skeletal deformations (Hanauer and Young 2002). The gene mutated in CLS patients (*RPS6KA3*) encodes a protein of 740 amino acids, RSK2 (alternative names: $p90^{RSK2}$, MAPKAPK1B), which belongs to a family of four highly homologous proteins (RSK1–4), encoded by distinct genes. RSKs are Ser/Thr protein kinases that act at the distal end of the mitogen-activated protein kinase/extracellular signal-regulated kinases (MAPK/ERK) signaling pathway. RSKs are directly phosphorylated and activated by ERK1/2 in response to many growth factors and neurotransmitters (Frödin and

Published online: 30 November 2010

Gammeltoft 1999). RSK2 phosphorylates a wide range of cytosolic substrates, such as GSK3 and IκB, and nuclear substrates including ATF4, c-FOS and NUR77, CREB and histone H3 (De Cesare et al. 1998; Sassone-Corsi et al. 1999). Activation of RSK2 is, therefore, thought to influence gene expression and to be involved in cell proliferation and survival. Numerous studies implicate the MAPK/ERK signaling cascade and CREB-mediated gene transcription in synaptic plasticity and memory (Davis and Laroche 2006). In human and mouse brain, RSK2 is highly expressed in the hippocampus, that is, an essential brain structure in cognitive function and learning (Zeniou et al. 2002; Guimiot et al. 2004). RSK2-deficient mice show delayed acquisition of a spatial memory reference task and long-term spatial memory deficits (Poirier et al. 2007). Thus, together the data suggest that RSK2 plays an important role in cognitive function in human and in mice.

To gain greater insight into the molecular mechanisms leading to learning and memory impairments in the *Rsk2*-KO mice and to mental retardation in CLS, we examined in the present study global gene expression profiles in hippocampus from KO mice. The data revealed significant alteration of 100 genes acting in a great variety of biological pathway in *Rsk2*-KO hippocampi. We further investigated the function of one of these genes, *Gria2*, which showed a twofold up-regulation in mutant mice. *Gria2* encodes the subunit GLUR2 of the AMPA receptor (AMPAR). AMPARs are ligand-activated cation channels that mediate the fast component of excitatory postsynaptic currents in neurons of the central nervous system. The GLUR2 subunit controls AMPAR Ca^{++} permeability, and is involved in several forms of long-term synaptic plasticity. Our results show that the expression of GLUR2 is increased at the mRNA and at the protein level in the hippocampus, as well as at the surface of synapses in hippocampal primary cell cultures. Furthermore, basal excitatory synaptic transmission through AMPARs is impaired in the hippocampus of *Rsk2* mutants.

Materials and methods

Animals and tissue dissection

Male *Rsk2*-KO and WT mice with a C57Bl/6x genetic background were killed by cervical dislocation. Brains were rapidly dissected and the hippocampus was isolated using a standard dissection procedure. Tissue samples were immediately frozen in liquid nitrogen and kept at −80°C until use. All experiments were carried out in accordance with the European Communities Council Directive of 24th November 1986 (86/609/EEC). Every effort was made to minimize the number of animals used and their suffering.

Microarray hybridization

To reduce variability, but also to obtain enough RNA for the hybridization of each DNA chip, all probes for the gene array experiments consisted of pooled RNA samples from either two WT or two KO animals. In brief, total RNA was extracted from hippocampi of six KO and six WT 5-month-old male mice and purified using the TRIzol reagent (Invitrogen, Cergy Pontoise, France) according to the manufacturer's instructions. The quality of total RNA was monitored by Agilent 2100 Bioanalyzer (LabChip, Agilent technologies, Massy, France). Two RNA samples for each genotype were then pooled in equal quantities (thus, resulting in a total of three arrays for each genotype). Generation of double-stranded cDNA from 2.5 µg of total RNA of each pooled RNA sample, preparation and labeling of cRNA, hybridization to 430A 2.0 mouse genome arrays (Affymetrix, Santa Clara, CA), washing, and scanning were performed according to the protocols recommended by Affymetrix in their GeneChip® Expression Analysis Technical Manual (Affymetrix). The data of the expression arrays produced for this report have been deposited in the Gene Expression Omnibus (GEO) databank.

Microarray data analysis

Data were processed using the Affymetrix GeneChip Operating Software [GCOS v1.4; Microarray Suite (MAS 5.0) algorithm]. Genes differentially expressed were selected using the following steps: (1) selection of probesets having a signal value above 15 (35th percentile of all expression values) in at least one array out the 6, (2) selection of probesets called present in at least two out of three arrays for one of the two genotypes, (3) selection of probesets with a t test $p < 0.03$, (4) selection of probesets having a fold change greater than 1.5. We finally verified that selected probes have acceptable false discovery rate (10%) (Benjamini and Hochberg 1995).

Ingenuity pathways analysis

Biologically relevant networks were created using the ingenuity pathways analysis program (http://www.Ingenuity.com), using the default parameters. Based on the algorithmically generated connectivity between gene–gene, gene–protein, and protein–protein interactions, the program develops functional molecular networks that overlay genes in the dataset. This program calculated p values for each network by comparing the number of focus genes that were mapped in a given network, relative to the total number of occurrences of those genes in all networks. The score for each network is shown as the negative log of the p value, which indicates the likelihood of finding a set of genes in the

network by random chance. A score of 20 indicates that there is a 10^{-20} chance that the focus genes would be in a network because of random chance.

Real-time QRT-PCR analysis

QRT-PCR assays were performed on hippocampal RNA samples obtained from WT and KO mice different from those used for transcriptional profiling. RNA extraction and QRT-PCR was performed as previously described (Marques Pereira et al. 2008). A probe set for detection of mouse *Gapdh* was used as an endogenous control gene. The sequences of primers of the tested genes are listed in Supplemental Table 1.

Western blot analysis

Protein extractions and Western blot analyses were performed as previously described (Marques Pereira et al. 2008). Quantifications were carried out with the GeneTool software of the Chemigenius apparatus (Syngene, Frederick, MD, USA). Data were normalized either to GAPDH or to β-TUBULIN. Student's t test (two-tailed) was used to determine the significance between the control and *Rsk2*-KO samples, and $p \leq 0.05$ was considered significant. Antibodies against GLUR2 (Millipore Corporation), CACNG8 and VAMP4 (Abcam), EIF3A (Cell Signaling Technology), DIABLO (Calbiochem), GAPDH (Chemicon) and β TUBULIN (Millipore) were used.

Immunohistochemistry

Frozen brain section was left 10 min at room temperature, fixed for 10 min with 4% PFA and washed twice (1× PBS). Endogenous peroxidase was inhibited by a treatment with 0.3% H_2O_2 solution. After washing, slides were incubated in 10% normal goat serum in 1× PBS for 1 h. Primary antibodies were added to the sections in 10% normal goat serum and incubated overnight at 4°C. Antibody dilutions were as follows: rabbit anti-GLUR2 (1:1000, Millipore Corporation), rabbit anti-VAMP4 (1:1,000, Abcam), and rabbit anti-IGF-1 (1:100, Abcam). Slides were subsequently washed four times for 10 min in 1× PBS and incubated with biotinylated secondary antibody for 2 h. After washing, sections were incubated for 30 min in Vectastain elite ABC reagent and treated with peroxidase substrate solution until desired stain intensity. After washing, samples were mounted with KAISER's glycerol gelatin (Merck).

In situ hybridization

Plasmids containing 3′UTR regions of mouse *Gria1* (encoding GLUR1) or *Gria2* (encoding GLUR2) cDNAs were amplified by PCR using vector-specific primers and PCR reactions were purified using Montage 96 (Millipore Corporation, Bedford, USA). Amplicons were then used as template for in vitro transcription of sense and anti-sense Dig-labeled riboprobes. To this aim, 1 µg linearized DNA was transcribed using T7, T3 or Sp6 polymerases and the 10× DIG RNA labeling mix (Roche Diagnostics, Meylan, France) according to the manufacturer's instructions. Brain sections 25-µm thick were processed for ISH using GenePaint robotic equipment and procedures (http://www.genepaint.org) as previously described (Nakamoto et al. 2007).

Primary hippocampal cultures

Hippocampi dissected from WT and *Rsk2*-KO male mice at embryonic day 17 were triturated and plated into wells of 24-well plates containing poly-D-lysine-coated coverslips (Sigma), at a density of ~1,00,000 neurons/well. Growth media consisted of NeuroBasal (GIBCO, Invitrogen) supplemented with 1× B27 (GIBCO, Invitrogen), 0.5 mM L-glutamine and 1× penicillin/streptomycin. The cultures were maintained at 37°C in a humidified atmosphere containing 5% CO_2 and cultivated for 14 DIV prior to experimentation.

Immunocytochemistry

To label surface GLUR1 (sGLUR1) and GLUR2 (sGLUR2)-containing AMPARs, 14 DIV live neurons were treated as previously described (Ghate et al. 2007) with minor modifications. Cells were incubated with rabbit anti-N-terminal GLUR1 (Calbiochem) or mouse anti-N-terminal GLUR2 (Millipore) and mouse anti-PSD95 (NeuroMab).

Microscopy and data analysis

All images acquisitions and quantifications were performed using standardized settings on a microscope (model DM4000 B, Leica) equipped with CCD camera (CoolSnap CF, color) with a ×63 objective. Obtained Tiff files were subjected to quantification with ImageJ software (http://www.rsb.info.nih.gov/ij/). For sGLURs quantification, the three thickest dendrites per pyramidal neuron and five neurons per sample were blindly chosen and the dendritic branches were manually traced and measured. AMPA receptors clusters were counted and the number of clusters was normalized with the dendritic length. Student's t tests were used for comparison between WT and *Rsk2*-KO cultures.

Determination of relative *Gria2* Q/R and R/G editing, and flip/flop splice levels

Total RNA was extracted (as above) from five *Rsk2*-KO and five WT hippocampi, the *Gria2* mRNA amplified by

RT–PCR (three times each from independent RNA preparations) and the product sequenced to determine the relative levels of editing and splicing (Lee et al. 1998).

Electrophysiology

Standard techniques were used to prepare transverse acute hippocampal slices (400-μm thick) from 4-week-old mice. Slices were maintained at room temperature in a storage chamber that was perfused with an artificial cerebrospinal fluid (ACSF) (mM: 119 NaCl, 2.5 KCl, 1.3 $MgSO_4$, 2.5 $CaCl_2$, 1 NaH_2PO_4, 26 $NaHCO_3$ and 11 glucose and equilibrated with 95% O_2 and 5% CO_2) for at least 1 h prior to recording. For synaptic recordings, a cut was made between the CA3 and CA1 region to prevent bursting, and the slices were bathed in a modified ACSF containing 100-μm picrotoxin to block GABAAreceptor- mediated inhibitory postsynaptic currents. Field excitatory postsynaptic potentials (fEPSPs) were recorded with glass pipettes (2–5 MΩ) filled with ACSF, by stimulating Schaffer collaterals in stratum radiatum (0.1 Hz) with a monopolar stimulating electrode. Responses were collected with Axopatch-1D amplifier (Axon Instruments), filtered at 2 kHz, digitized at 10 kHz, and analyzed online using Clampfit software (Molecular Devices).

Results

Expression profiling of wild-type and *Rsk2*-KO mice

To identify molecular changes potentially responsible for the phenotype associated with *RSPS6KA3* gene mutation in the hippocampus, we performed a detailed comparison of the transcriptional profiles of hippocampi isolated from six KO and six WT 5-month-old male mice. To reduce variability, equivalent amounts of RNA from two mice with the same genotype were pooled and processed for hybridization to the genome wide oligonucleotide microarray (thus, three arrays per genotype). Out of the 22,690 probesets represented on the microarray, filter A selected 16,865 probesets that were restricted to 14,348 probesets by filter b and to 635 probesets by filter c. Filter d, selected a final number of 109 probesets. Eight of these 109 differentially expressed genes were verified by two or, in one case, three distinct probe sets. These multiple probe sets of eight genes displayed consistent direction and similar extent of changes in abundances of corresponding mRNAs. The final list of 100 significant non-redundant genes is shown in Table 1. Genes are tabulated according to functional category and degree of over-expression/repression.

Most of them have a recognized function and can be assigned to functional categories and subcategories. Among them, 75 genes were transcriptionally up-regulated, whereas 25 genes were down-regulated. The most upregulated genes were thymosin beta 10 (*Tmsb10*, fold change of 3.51), followed by establishment of cohesion 1 homolog A (*Esco 1*, fold change of 2.91) and thyroid hormone receptor interactor 11 (*Trip 11*, fold change of 2.27). The most downregulated genes were erythroid differentiation regulator 1 (*Erdr1*) and serpin peptidase inhibitor, clade C, member 1 (*Serpin1*) (−2.9 and −2.4 fold downregulations, respectively). Major functional categories include enzymes with various activities (17 up-regulated/2 down-regulated), growth factors (2/0), ion channels (3/0), kinases (1/3), peptidases (2/1), transcription regulators (6/1), transmembrane receptors (1/0), transporters (7/2) and molecules with other functions (33/14).

Validation of microarray data by QRT-PCR

Twenty-four of these differentially expressed genes were selected for validation, by QRT-PCR, based on the known or putative neuronal functional roles (Table 1). These genes represent different categories: genes implicated in exocytosis (*Stxbp3* and *Vamp4*), in mental retardation (*Cul4b*, *Lamp2*, *Vldlr, Igf1*), in apoptosis (*Stk3*, *Rasl10a*, *Diablo*), in cell differentiation and cytoskeleton organization (*Phkg1*, *Pdlim5*, *Timsb10*, *Enc1*, *Nptxr*, *Ptpn2*, *Carhsp1*, *Phip*, *Plek*, *Arhgap12*, *Cfl1*), in translation regulation (*Eif3A*) and finally genes encoding ion channel sub-units (*Cacnb4*, *Cacng8*, *Gria2*). The results of the microarray findings were validated in all the genes tested by real-time PCR, although the fold change was not always accurately replicated. We also confirmed by QRT-PCR unaltered expression of some genes (including cFos, CREB) that had similar levels of expression in KO and WT animals on microarrays (results not shown).

Identification of biologically relevant networks

To gain insight into interactions among the differentially expressed genes, we constructed biologically relevant networks using the ingenuity pathway analysis software. From the 100 differentially expressed genes, 78 genes were mapped and assembled into five biological networks with a score of $\geq$20. The network with the most significant score (of 45) contains 23 of the differentially expressed genes. This network contains genes involved in cell cycle, cellular development, growth and proliferation and centers on the NFκB complex. This network contains also Rb1 and Sod2, both important actors in cellular growth and apoptosis, and over expressed in *Rsk2*-KO neurons. The network with the second highest score (of 34) is centered on TGFβ1, which controls proliferation, cellular differentiation, but also various other functions. Fourteen genes with altered

Table 1 List of genes differentially expressed in the hippocampus of Rsk2-KO mice

Functional category	Probe set	Genbank	Gene symbol	Gene name	Microarray		qRT-PCR			
					F C KO/WT	*p*	WT mean Ct ± SD	KO mean Ct ± SD	FC	*p*
Genes showing decreased expression										
Kinases	1422315_x_at	NM_011079	*Phkg1*	Phosphorylase kinase gamma 1	0.54	0.0162	1 ± 0.03	0.68 ± 0.11	0.68	0.003
	1418052_at	NM_023556	*Mvk*	Mevalonate kinase	0.55	0.0190				
	1427282_a_at	NM_008044	*Fxn*	Frataxin	0.61	0.0074				
Enzymes	1448330_at	NM_010358	*Gstm5*	Glutathione *S*-transferase M5	0.61	0.023				
	1427975_at	NM_145216	*Rasl10a*	Ras-like, family 10, member A	0.62	0.015	1 ± 0.05	0.70 ± 0.059	0.70	0.004
Peptidase	1433918_at	NM_034941	*Atg4d*		0.59	0.0057				
Cytokine	1418345_at	NM_023517	*Tnfsf13*	Tumor necrosis factor (ligand) superfamily, member 13	0.60	0.0057				
Transcription regulator	1418636_at	NM_001083318	*Etv3*	Ets variant gene 3	0.55	0.026				
Transporters	1423927_at	NM_028662	*Slc35b2*	Solute carrier family 35, member B2	0.59	0.011				
	1450073_at	NM_008444	*Kif3b*	Kinesin family, member 3B	0.64	0.00093				
Transmembrane receptor	1450147_at	NM_030689	*Nptxr*	Neuronal pentraxin receptor	0.62	0.013	1 ± 0.008	0.87 ± 0.35	0.87	0.035
Other functions	1452406_x_at	NM_133362	*Erdr1*	Erythroid differentiation regulator 1	0.35	0.029				
	1417909_at	NM_080844	*Serpinc1*	Serpin peptidase inhibitor, clade C, member 1	0.41	0.023				
	1415976_a_at	NM_025821	*Carhsp1*	Calcium regulated head stable protein 1,24 kDa	0.50	0.00036	1 ± 0.07	0.63 ± 0.07	0.63	0.034
	1452652_a_at	NM_001002267	*Tmem158*	Transmembrane protein 158	0.55	0.015				
	1448577_x_at	NM_009304	*Syngr2*	Synaptogyrin 2	0.56	0.021				
	1455098_a_at	NM_011707	*Vtn*	Vitronectin	0.57	0.0022				
	1453111_a_at	NM_026542	*Slc25a39*	Solute carrier family 25, member 39	0.61	0.011				
	1418396_at	NM_134116	*Gpsm3*	G-protein signaling modulator 3	0.63	0.016				
	1423940_at	NM_026553	*Yif1A*	Yip1 interacting factor homolog A (*S. cerevisiae*)	0.63	0.016				
	1418123_at	NM_011676	*Unc119*	Unc-119 homolog (*C. elegans*)	0.64	0.0016				
	1450468_at	NM_010865	*Myoc*	Myocilin	0.64	0.0078				
	1415886_at	NM_013781	*Sh2d3c*	SH2 domain containing 3C	0.64	0.001				
	1422596_at	NM_021426	*Nkain4*	Na+/K+ transporting ATPase interacting 4	0.65	0.022				
	1450255_at	NM_020260	*Cdgap*	Cdc42 GTPase-activating protein	0.65	0.009				
Genes showing increased expression										
Kinases	1418513_at	NM_019635	*Stk3*	Serine/threonine kinase 3	1.76	0.023	1 ± 0.05	1.45 ± 0.08	1.45	0.042
Phosphatase	1438562_a_at	NM_001127177	*Ptpn2*	Protein tyrosine phosphatase, non-receptor type 2	1.95	0.016	1 ± 0.091	1.85 ± 0.28	1.83	0.045
Growth factors	1437401_at	NM_010512	*Igf1*	Insulin-like growth factor 1	1.65	0.0093	1 ± 0.09	2.24 ± 0.32	2.24	0.042
	1417069_a_at	NM_022023	*Gmfb*	Maturation factor, beta	1.54	0.0055				

Table 1 continued

Functional category	Probe set	Genbank	Gene symbol	Gene name	Microarray		qRT-PCR			
					F C KO/WT	*p*	WT mean Ct ± SD	KO mean Ct ± SD	FC	*p*
Enzymes	1448734_at	NM_001042611	*Cp*	Ceruloplasmin	2.29	0.029				
	1417262_at	NM_011198	*Ptgs2*	Prostaglandin-endoperoxidase synthase 2	2.28	0.0047				
	1452484_at	NM_053070	*Ca7*	Carbonic anhydrase VII	2.23	0.028				
	1417194_at	NM_013671	*Sod2*	Superoxide dismutase 2	1.98	0.0089				
	1452158_at	NM_029735	*Eprs*	Glutamyl-prolyl-tRNA synthetase	1.95	0.015				
	1453928_a_at	NM_009278	*Ssb*	Sjogren syndrome antigen B	1.86	0.020				
	1451436_at	NM_001081203	*Sbno1*	sno, strawberry notch homolog 1 (*Drosophila*)	1.78	0.022				
	1454696_at	NM_008142	*Gnb1*	Guanine nucleotide binding protein, beta polypeptide 1	1.70	0.0016	1 ± 0.033	1.36 ± 0.061	1.36	0.0005
	1419064_a_at	NM_011674	*Ugt8*	UDP-glycosyltransferase 8	1.69	0.0059				
	1416497_at	NM_009787	*Pdia4*	Protein disulfide isomerase family A, member 4	1.68	0.0061				
	1423033_at	NM_008408	*Stt3a*	Subunit of the oligosacchayltransferase complex, homolog A	1.66	0.028				
	1435164_s_at	NM_011666	*Ube1c*	Ubiquitin-activating enzyme E1C	1.65	0.0062				
	145388_at	NM_183028	*Pcmtd1*	protein-L-isoaspartate *O*-methyltransferase domain containing 1	1.60	0.026				
	1416343_a_at	NM_010685	*Lamp2*	Lysosomal-associated membrane protein 2	1.58	0.023	1 ± 0.05	1.65 ± 0.19	1.65	0.038
	1418908_at	NM_013626	*Pam*	Peptidylglycine alpha-amidating monooxygenase	1.56	0.021				
	1451828_a_at	NM_207625	*Acsl4*	Acyl-CoA synthetase long chain family member 4	1.54	0.0035				
	1417697_at	NM_009230	*Soat1*	Sterol *O*-acyltransferase	1.51	0.015				
Peptidase	1420964_at	NM_007930	*Enc1*	Ectodermal-neural cortex	2.07	0.015	1 ± 0.05	1.77 ± 0.08	1.77	0.002
	1449718_s_at	NM_026273	*C3orf38*	Chromosome 3 open reading frame 38 homolog (human)	1.54	0.019				
Transcription regulators	1427406_at	NM_028446	*Trip11*	Thyroid hormone receptor interactor 11	2.27	0.0045				
	1423501_at	NM_008558	*Max*	MYC-associated factor X	1.91	0.023				
	1417187_at	NM_016786	*Hip2*	Huntington interacting protein 2	1.76	0.0071				
	1424704_at	NM_001145920	*Runx2*	Runt-related transcription factor 2	1.67	0.0068				
	1418265_s_at	NM_008391	*Irf2*	Interferon regulatory factor	1.60	0.023				
	1417850_at	NM_009029	*Rb1*	Retinoblastoma 1	1.58	0.0053				
Translation regulator	1416661_at	NM_010123	*Eif3a*	Eukaryotic translation initiation factor 3, subunit A	1.74	0.0087	1 ± 0.05	1.84 ± 0.11	1.84	0.005
Nuclear receptors	1422631_at	NM_013464	*Ahr*	Aryl hydrocarbon receptor	1.61	0.028				
	1416958_at	NM_011584	*NriD2*	Nuclear receptor subfamily 1, group D, member 2	1.54	0.0064				
Transporters	1422966_a_at	NM_011638	*Tfrc*	Transferrin receptor	2.10	0.0010				
	1416653_at	NM_011504	*Stxbp3*	Syntaxin-binding protein 3	1.92	0.013	1 ± 0.03	2.19 ± 0.6	2.19	0.038
	1442169_at	NM_013703	*Vldlr*	Very low density lipoprotein receptor	1.79	0.0068	1 ± 0.05	1.44 ± 0.055	1.44	0.0007
	1424924_at	NM_153055	*Sec63*	SEC63 homolog (*S. cerevisiae*)	1.74	0.015				
	1419975_at	NM_011327	*Scp2*	Sterol carrier protein 2	1.66	0.023				
	1416374_at	NM_018829	*Ap3m1*	Adaptor-related protein complex 3 mu 1 subunit	1.59	0.0032				
	1434513_at	NM_001128096	*Atp13a3*	ATPase type 13A3	1.52	0.0054				
Ion channels	1453098_at	NM_013540	*Gria2*	Glutamate receptor, ionotropic, AMPA2	2.01	0.024	1 ± 0.032	1.87 ± 0.09	1.87	0.0003
	1452089_at	NM_001037099	*Cacnb4*	Calcium channel, voltage-dependent, beta 4 subunit	1.85	0.0031	1 ± 0.022	1.34 ± 0.02	1.34	0.022
	1451864_at	NM_133190	*Cacng8*	Calcium channel, voltage-dependent, gamma subunit 8	1.79	0.012	1 ± 0.08	1.84 ± 0.26	1.84	0.005

Table 1 continued

Functional category	Probe set	Genbank	Gene symbol	Gene name	Microarray		qRT-PCR			
					F C KO/WT	*p*	WT mean Ct ± SD	KO mean Ct ± SD	FC	*p*
Other functions	1455946_x_at	NM_001039392	*Tmsb10*	Thymosin, beta 10	3.51	0.0052	1 ± 0.04	2.56 ± 0.05	2.56	0.028
	1424325_at	NM_001081222	*Esco1*	Establishment of cohesion 1 homolog 1 (*S. cerevisiae*)	2.91	0.024				
	1425768_at	NM_023232	*Diablo*	Diablo homolog (*Drosophila*)	2.05	0.023	1 ± 0.032	2.16 ± 0.05	2.16	0.0002
	1455475_at	NM_026622	*C4orf29*	Chromosome 4 open reading frame 29 homolog (human)	2.00	0.023				
	1423198_a_at	NM_134034	*Smek2*	SMEK homolog 2, suppressor of mek1 (Dictyostelium)	1.93	0.014				
	1424074_at	NM_027453	*Btf3l4*	Basic transcription factor 3-like 4	1.88	0.018				
	1420485_at	NM_023554	*Nol7*	Nucleolar protein 7	1.78	0.016				
	1438418_at	NM_144535	*Mudeng*	MU-2/AP1M2 domain containing, death-inducing	1.77	0.014				
	1421945_a_at	NM_001042556	*Bxdc1*	Brix domain containing 1	1.77	0.0077				
	1450418_a_at	NM_026553	Yif1a	Yip1-interacting factor homolog A (*S. cerevisiae*)	1.74	0.029				
	1449884_at	NM_026626	Efcab2	EF-hand calcium binding domain 2	1.71	0.020				
	1418008_at	NM_026110	C21orf66	Chromosome 21 open reading frame 66 homolog (human)	1.68	0.023				
	1438535_at	NM_001081216	Phip	Pleckstrin homology domain interacting protein	1.65	0.011	1 ± 0.19	2.08 ± 0.09	2.08	0.03
	1451525_at	NM_001039692	Arhgap12	Rho GTPase-activating protein 12	1.64	0.020	1 ± 0.09	1.54 ± 0.09	1.54	0.033
	1426271_at	NM_153808	Smc5	Structural maintenance of chromosome 5	1.63	0.015				
	1417170_at	NM_033322	Lztfl1	Leucine zipper transcription factor-like 1	1.62	0.029				
	1452247_at	NM_001113188	Fxr1	Fragile X mental retardation, autosomal homolog 1	1.62	0.0047				
	1451325_at	NM_027226	Fyttd1	Forty-two–three domain containing 1	1.61	0.0050				
	1425913_a_at	NM_144882	Dnaptp6	Viral DNA polymerase-trans-activated protein 6	1.60	0.012				
	1421940_at	NM_009282	Stag1	Stromal antigen 1	1.59	0.011				
	1448748_at	NM_019549	Plek	Pleckstrin	1.58	0.021	1 ± 0.05	1.12 ± 0.09	1.12	0.004
	1451830_a_at	NM_009260	Spnb2	Spectrin, beta, non-erythrocytic 1	1.58	0.019				
	1437463_x_at	NM_011577	TgfbI	Transforming growth factor, beta-induced	1.57	0.016				
	1423841_at	NM_026396	Bxdc2	Brix domain containing 2	1.57	0.026				
	1427104_at	NM_175480	Znf23	Zinc finger protein 612	1.56	0.015				
	1426806_at	NM_028696	Obfc2a	Oligonucleotide/oligosaccharide-binding fold containing 2A	1.55	0.023				
	1422896_at	NM_016796	Vamp4	Vesicle-associated membrane, protein 4	1.55	0.016	1 ± 0.07	1.48 ± 0.16	1.48	0.034
	1437790_at	NM_001081191	Eml5	Echinoderm microtubule associated protein like 5	1.54	0.020				
	1417453_at	NM_001110142	Cul4b	Cullin 4B	1.53	0.028	1 ± 0.03	1.12 ± 0.09	1.12	0.018
	1418066_at	NM_007688	Cfl2	Cofilin 2	1.53	0.019				
	1450407_a_at	NM_009672	Anp32a	Acidic nuclear phosphoprotein 32 family, member A	1.53	0.013				
	1450786_at	NM_019808	Pdlim5	PDZ and LIM domain 5	1.53	0.0057	1 ± 0.11	1.44 ± 0.059	1.44	0.047
	1425597_a_at	NM_021881	Qk	Quaking homolog, KH domain RNA binding	1.52	0.029				

Real-time quantitative RT–PCR was performed for 24 genes in hippocampi of *Rsk2*-KO ($n = 6$) and WT ($n = 6$) mice, using the primer pairs shown in Table S1. Relative expression levels are shown with the average expression value of the WT group set to 1

Ct cycle threshold values, *SD* standard deviation, *FC* fold change, *p p* value

expression in *Rsk2*-KO mice are associated with this second network, among which Nptxr, Cacng8, Pdlim5 and Soat1. The third network centered on MYC is mainly implicated in lipid metabolism and cell death. Thirteen focus genes are associated with this network, including Acsl4, Eif3a, Ca7, Cfl2 and Fxr1. The last two networks are mainly implicated in molecular transport and lipid metabolism (4th network) and amino acid metabolism and protein synthesis (5th network). The fourth network is centered on Ptgs2 and includes 12 focus genes, among which Igf1, Vamp4, Mvk, Stxbp3 and Gnb1. The fifth network is centered on retinoic acid and contains 13 focus genes, among which Cacnb4 and Carhsp1. Figure 1 shows the two most significant networks (the others are available on request to AH). Supplemental Table 2 lists the top related biological functions and diseases. Top biological functions include organismal injury and abnormalities (9 genes, including Fxn, Sod2, Igf1, Ahr and Ptgs2), cell cycle (12 genes including Rb1, Igf1 and Runx2), nervous system development and function (10 genes including Igf1, Ptgs2, Sod2, Gria2, Vldlr, Vtn and Rb1), organismal development and free radical scavenging (9 and 4 genes, respectively). Interestingly, five genes, including Gria2, Igf1, Ptgs2, Sod2 and Vldlr have been implicated in behavior, with the first four genes specifically in spatial memory formation. These five genes are all up-regulated in the hippocampus of *Rsk2*-KO mice. The p values in the range of 2.52×10^{-5} to 1.10×10^{-2} indicate statistical significance.

Confirmation of altered expression at the protein level

We confirmed increased expression at the protein level of GLUR2 (*Gria2* gene), CACNG8, VAMP4, EIF3A and DIABLO using quantitative western blot analysis (Fig. 2). These findings are in line with the changes detected by microarray-based analysis. We also confirmed differential expression of GLUR2, VAMP4 and IGF1 using immunohistochemical analysis. As shown in Fig. 3, we found increased expression of GLUR2 in the CA1 and CA3 regions and in the dentate gyrus of *Rsk2*-KO hippocampus. VAMP4 and IGF1 were increased in the whole hippocampus. Although the lack of specific antibodies precluded similar experimental validations for many other genes listed in Table 1, these observations suggested that the transcriptional changes observed in mutant mice may be generally reflected by matching changes in the levels of expression of their corresponding protein products.

Confirmation by in situ hybridization of Gria2 up-regulation

The expression of a number of genes involved in neurotransmission, including vesicle and receptor trafficking proteins, neurotransmitter receptors and ion channels, were altered in *Rsk2*-KO mice (Table 1). Of particular interest was the twofold increased level of expression of *Gria2*, encoding the subunit GLUR2 of the AMPAR. Since AMPARs mediate fast synaptic transmission at excitatory synapses in the brain and are thought to play key roles in synaptic plasticity, learning and memory (Seidenman et al. 2003) we wanted to further confirm up-regulation of the *Gria2* gene by in situ hybridization of WT and KO mice hippocampi. The expression of *Gria2* was significantly increased in all areas of the anterior hippocampus of mutant mice (Fig. 4a), whereas in the posterior hippocampus, the level of *Gria2*-mRNA was mainly increased in the dentate gyrus, in CA1 and in the CA3 region (Fig. 4b). We did not find any change in the level of expression of GLUR1 (not shown).

Increase in GLUR2 surface expression

We next wondered whether expression of GLUR2 at surface of synapses was also up-regulated since AMPARs in hippocampal neurons are mainly expressed as heteromers of GLUR1/2 as well as GLUR2/3. We compared the amount of GLUR2 at synapses in KO and WT cultured primary hippocampal neurons by staining surface GLUR2 (or GLUR1) clusters and counterstaining for PSD95. GLUR2 surface staining was punctate (Fig. 5a, b), and the number of GLUR2 puncta that were synaptic did significantly differ among WT and *Rsk2*-KO cultures (WT 8.1 ± 1.4, $n = 12$ embryos, KO 14.9 ± 2.2, $n = 12$, $p = 0.015$). This provided evidence that increase in total GLUR2 was correlated with increased surface-expressed GLUR2. No significant difference of surface GLUR1 was detected (WT 12.4 ± 7.4, $n = 4$, KO 10.7 ± 5, $n = 6$, $p = 0.8$) (Supplemental Fig. 1).

Determination of relative *Gria2* R/G editing and flip/flop splice levels

The great majority of native AMPA receptors are impermeable to calcium ions, due to the presence of the GLUR2 subunit. This subunit confers calcium impermeability on the channel due to RNA editing of a glutamine (Q) to an arginine (R) at codon 607. In addition to the Q/R site in GLUR2, the GLUR2, 3 and 4 subunits undergo RNA editing (arginine to glycine) at codon 764 (in GLUR2) (Lomeli et al. 1994). The pre-messenger RNA transcripts of all the four GLUR subunits can finally be alternatively spliced to produce either the flip or flop isoforms. Because the level of expression of GLUR2 was increased in *Rsk2*-KO mice, we wondered whether *Gria2* RNA editing and splicing were altered.

To determine whether there are changes in the Q/R, R/G site editing and flip/flop splice levels of the *Gria2*

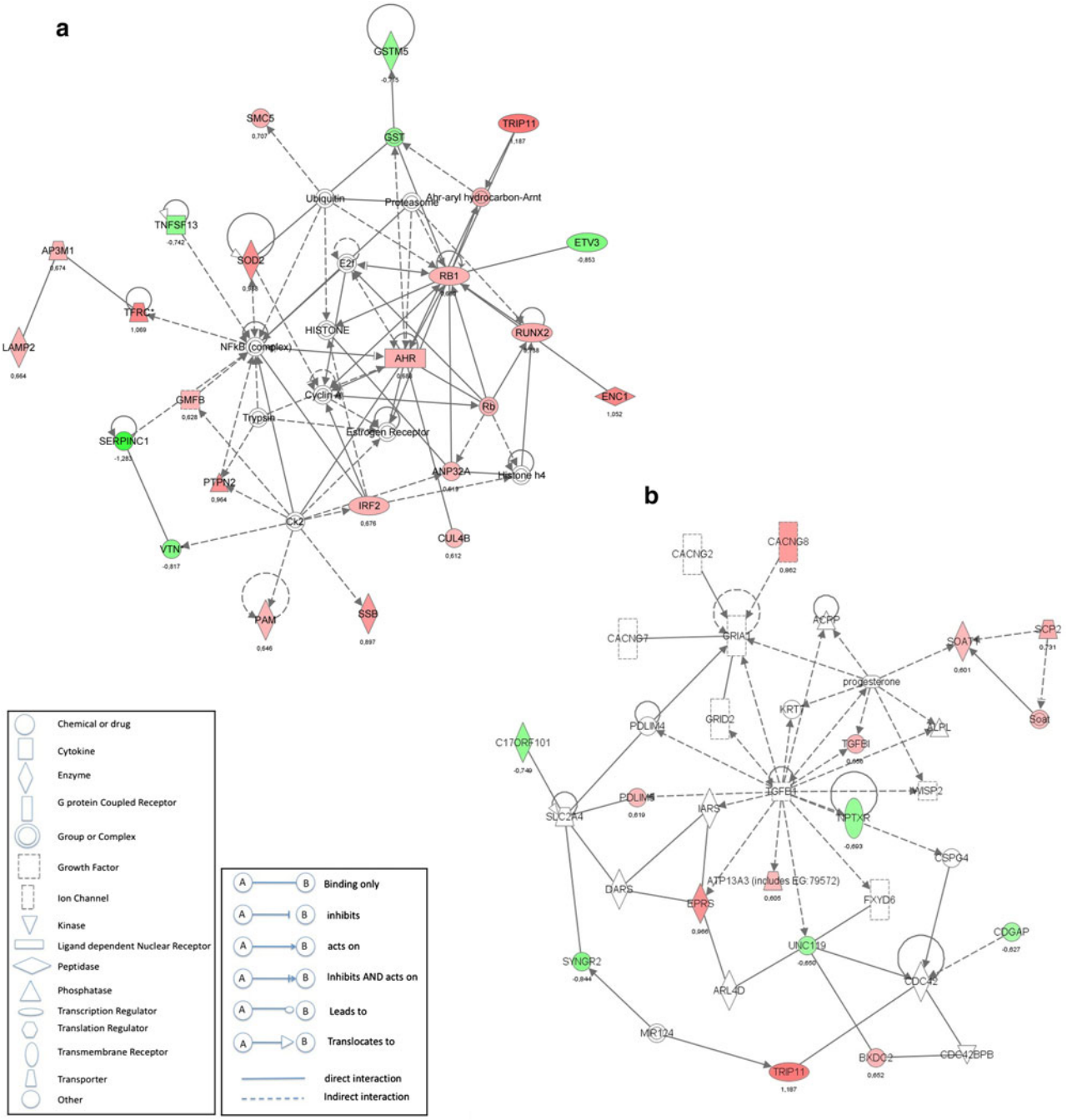

Fig. 1 Top integrated networks dysregulated in the hippocampus of *Rsk2*-KO. Networks were created by the Ingenuity Pathway Analysis Software. Up-regulated genes are listed in *red* and down-regulated in *green*. **a** This network is centered on NFκB. Twenty-five differentially expressed focus genes were brought into this network with a score of 45. **b** This network is centered on TGFβ1. Fifteen differentially expressed focus genes were brought into this network with a score of 26. Nodes and edges are described below the networks

messenger in 5-month-old *Rsk2*-KO hippocampi, the *Gria2* mRNA from five *Rsk2*-KO and five WT hippocampi was amplified by RT-PCR and the products sequenced to determine the relative levels of editing and splicing (Lee et al. 1998). No unedited form of the *Gria2* transcript at the Q/R site (codon 607) was detectable (not shown) neither in KO nor in WT mice, suggesting that the amount is very low. These data are in accordance with the previously reported results indicating that editing of Q/R site is ~99% complete in postnatal brain (Carlson et al. 2000). At the R/G editing site (codon 764) edited (codon GGA) and unedited (codon AGA) forms were detectable in both WT and mutant mice.

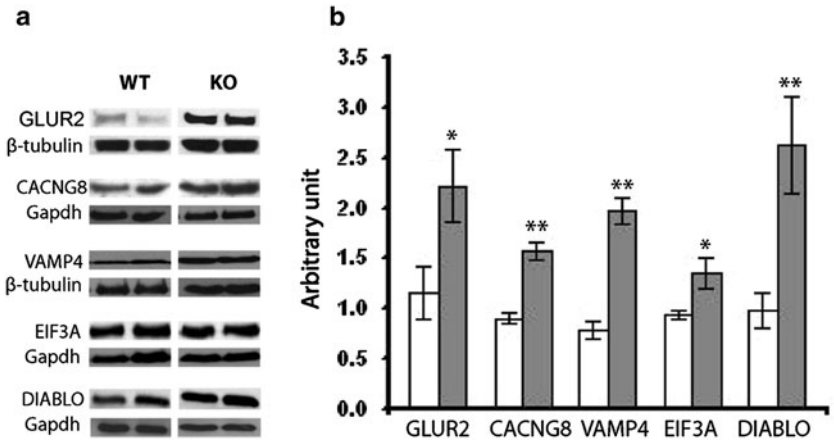

Fig. 2 Quantitative Western blot analyses. Levels of proteins expressed by the five up-regulated genes assayed are significantly increased in the hippocampus of *Rsk2*-KO mice. **a** Proteins detected in two *Rsk2*-KO and two WT mice are shown. **b** Data normalized either to GAPDH or to β-TUBULIN are represented as the mean ± SEM for six mice of each genotype for GLUR2 and CACNG8 and four mice for EIF3A, VAMP4 and DIABLO. *WT* white bar, *KO* gray bar $*p < 0.05$ and $**p < 0.01$

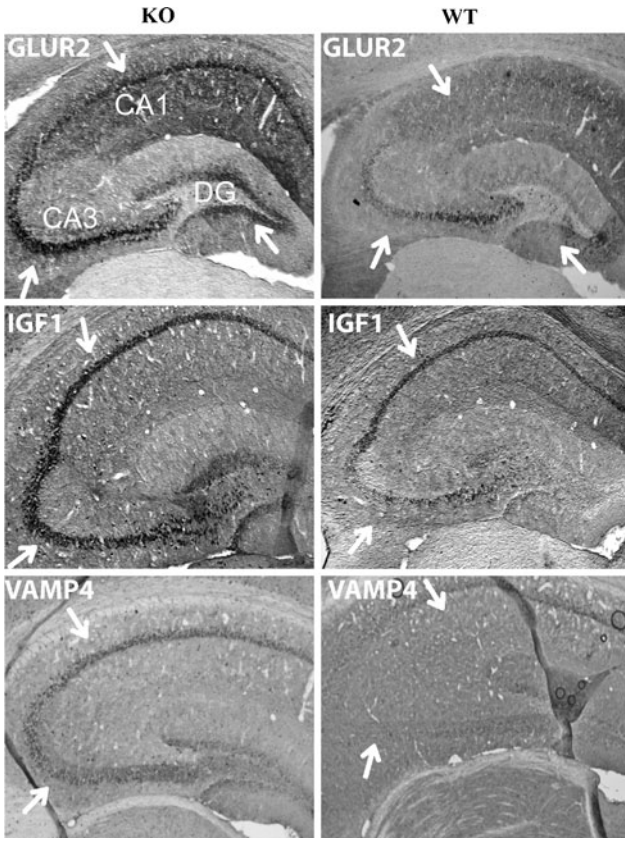

Fig. 3 Immunohistochemical analysis. Proteins expressed by three up-regulated genes show significantly higher expression in *Rsk2*-KO mice hippocampus. Three mice for each genotype were analyzed. Each *picture* represents one of the triplicates. *Arrows* point to hippocampus sub-regions showing increased expression in KO versus WT mice. CA1, CA3 and DG (dentate gyrus): hippocampus sub-regions

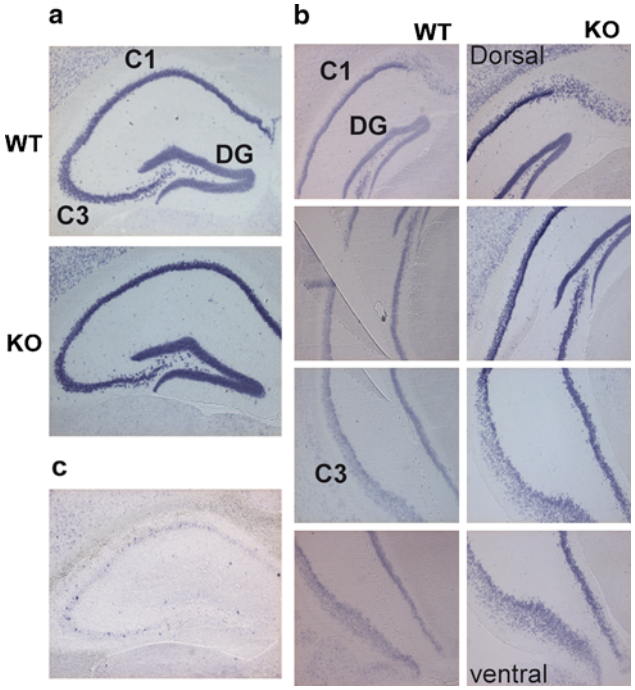

Fig. 4 In situ hybridization. Dig-labeled *Gria2* sense and anti-sense RNAs were hybridized to 25-µm coronal sections of three *Rsk2*-KO and three WT adult mouse brains. One *picture* from each genotype is shown. **a** Significantly increased expression in all areas of the anterior hippocampus of *Rsk2*-KO mice. **b** In the posterior hippocampus the level of *Gria2*-mRNA was mainly increased in the dentate gyrus, in CA1 and in the ventral CA3 region. **c** No staining was observed with sense RNA

The peak intensity of the G nucleotide signal at the edited position was measured and reported as a percentage of the total signal (A and G). Representative chromatograms from one KO and one WT littermate are shown in Supplementary Fig. 2. In WT hippocampi, the *Gria2* mRNA was approximately 61 ± 4% edited, whereas there was less editing in *Rsk2*-KO hippocampi (43 ± 3%, $p = 0.005$). Our data for WT mice are in accordance with the previous reports

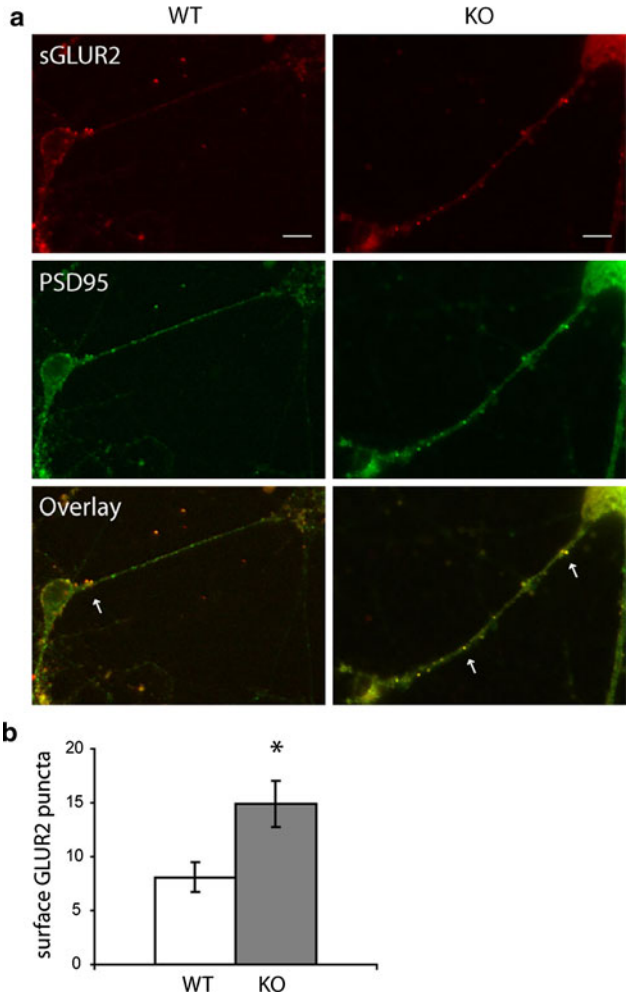

Fig. 5 Surface expression of AMPAR. **a** WT and *Rsk2*-KO hippocampal neurons were labeled with N-terminal GLUR2 antibody under non-permeabilized condition to stain surface GLUR2 (sGLUR2), followed by PSD95 staining (a post-synaptic marker). *Arrows* point to post-synaptic surface-expressed GLUR2. *Scale bar* 10 μm. **b** Quantification of sGLUR2 puncta. Data represent mean ± SEM of detected sGLUR2 clusters per unit dendrite length, from $n = 12$ (WT) and 12 (KO) embryos. $^*p < 0.05$

demonstrating an editing status at the R/G site of approximately 64% (Lai et al. 1997). Thus, in *Rsk2*-KO mice the extent of R/G editing was significantly decreased (rel. decrease: 18%, $p = 0.003$) in the hippocampal tissue.

To determine the ratio of transcripts in the flip/flop alternative splice form, the peak intensity of the first nucleotide difference (C vs. A) between the two variants was measured (Lee et al. 1998). In the WT hippocampi, there were approximately 55 ± 5% of Glur2 transcript in the flip form, whereas the percentage was significantly lower (43 ± 3%, $p = 0.002$) in the *Rsk2*-KO hippocampi (Supplemental Fig. 2c, d). No significant difference for the *Gria1* mRNA (encoding GLUR1) for the R/G editing site or flip/flop splice levels was found between WT and mutant mice (Supplemental Fig. 2a, b).

Reduced AMPA synaptic transmission

We then investigated whether changes in *Gria2* expression, editing and splicing affect basal AMPAR-mediated synaptic transmission in hippocampal slices from 4-week-old *Rsk2*-KO mice. To assess the strength of synaptic transmission, we compared the size of the presynaptic fiber volley (input) to the slope of the EPSP (output) in striatum radiatum and found a ~25% significant reduction in *Rsk2*-KO ($n = 9$) mice when compared with WT littermates ($n = 7$) (Fig. 6a). We evaluated also paired-pulse facilitation (PPF), a measure of release probability from presynaptic terminals. The PPF curves were essentially identical in slices from control and *Rsk2*-KO mice (Fig. 6b) indicating that RSK2 most likely modulates AMPA neurotransmission postsynaptically with no effect on presynaptic function.

Discussion

The absence of gross structural alterations in the brain of *Rsk2*-KO mice strongly indicates that their defective cognitive phenotype should be linked to subtler molecular or cellular alterations. In an effort to identify such alterations, we carried out a detailed characterization of the differences existing between the transcriptional profiles of the hippocampus of WT and KO animals. Our analysis by oligonucleotide microarrays yielded a list of 100 differentially expressed genes with high degree of statistical significance. These results were further confirmed for 24 genes by quantitative RT-PCR demonstrating their robustness.

Our study revealed a great variety of RSK2-influenced genes acting in various biological pathways. Indeed, the network with the highest score (as determined by ingenuity pathway analysis) centers on the NFκB complex, which plays a prominent role in cell differentiation and proliferation and apoptosis (Brand et al. 1997). Twelve genes are implicated at various stages of the cell cycle in *Rsk2*-KO neurons (including *Igf1, Rb1, Max, Sod2, and, Ptgs2*). This result suggests strongly that abnormal cell proliferation contributes to the CLS phenotype. In addition, 34 of the altered genes have been implicated in cell death or survival, out of which 7 (*Cacng8, Diablo, Gria2, Igf1, Ptgs2, Rb1, Sod2*) have been specifically associated with neuronal cell death. Interestingly, previous studies suggested that apoptotic and antiapoptotic cascades are tightly associated with cognitive dysfunctions and neurological disorders (Lutz 2007). Further studies are, therefore, necessary to investigate cell proliferation and death in *Rsk2*-KO mice. Four genes, including *Sod2, Fxn, Gmfb* and *Cp* are implicated in free radical scavenging, suggesting also a possible involvement of free radicals in the

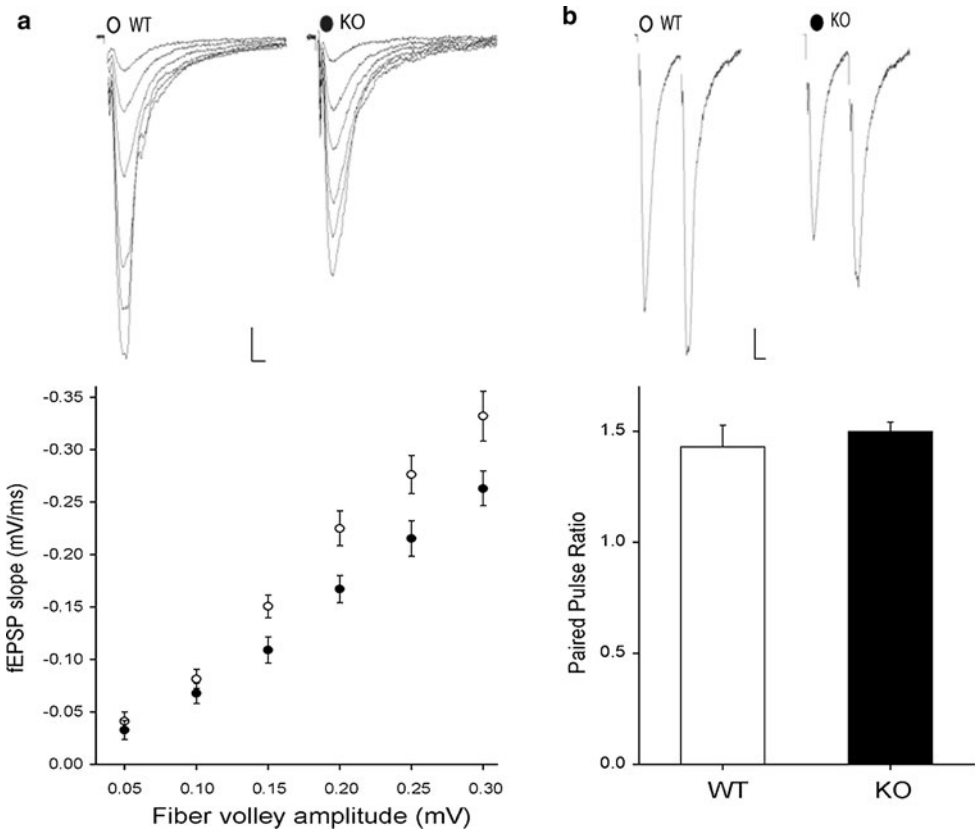

Fig. 6 Patch-clamp analysis**. a** Input–output curves for basal synaptic transmission in hippocampal slices. As illustrated in the sample traces and the *graph*, for each input (fiber volley $\geq$ 0.15 mV), the output (fEPSP) is reduced by 25% in *Rsk2*-KO slices ($p \leq 0.05$, WT $n = 10$; KO $n = 9$). *Scale bar* 0.1 mV, 5 ms. **b** Paired-pulse facilitation (PPF) does not differ between *Rsk2*-KO ($n = 9$) and WT ($n = 6$) cells. Sample traces are illustrated above the *bar graph*. *Scale bar* 0.05 mV, 10 ms

CLS phenotype. Ten genes (among which *Gria2, Igf1, Ptgs2, Sod2*, *Nptxr, Ahr* and *Vtn*) play a role in nervous system development and function. IGF1 for instance is essential for normal dendritic growth (Cheng et al. 2003). NPTXR is thought to be involved in activity-dependent synaptic plasticity (Xu et al. 2003). The AHR homologs in *Drosophila*, *Spineless* (*Ss*), and in *Caenorhabditis elegans*, *ahr-1*, regulate dendrite morphology (Kim et al. 2006) and neuronal differentiation (Qin and Powell-Coffman 2004). The expression of a number of genes involved in neurotransmission was also found affected. Up-regulation of the *Vamp4* and *Stxbp3* genes in mutant mice points to a role of RSK2 in pre-synaptic vesicle trafficking (Wang and Tang 2006). Up-regulation of *Cacnb4*, encoding a β-subunit of Voltage-gated Ca^{++} channels, suggests that influx of Ca^{++} into the cell upon membrane polarization is regulated via RSK2 (Birnbaumer et al. 1998). Moreover, alteration of *Gnb1* and *Gria2* expression suggests that RSK2 is involved in glutamate receptor signaling. GNB1 mediates the fast voltage-dependent inhibition of N-type Ca^{++} channels (Fu and Cheung 1999). The function of Gria2 will be discussed below. Finally, the expression of several genes encoding proteins implicated in gene expression was altered in *Rsk2*-KO hippocampi (including the transcription regulators *Etv3, Hip2, Rb1, Irf2, Max, Runx2* and *Trip11*) suggesting that some of the RSK2 effects may be direct and others indirect. Strikingly, two of the genes with altered expression in *Rsk2*-KO hippocampi, *Lamp2* and *Cul4b*, have previously been associated with syndromic forms of X-linked mental retardation (Nishino et al. 2000; Zou et al. 2007).

Among the genes associated with a specific neuronal function, *Gria2* was of particular interest because GLUR2 controls the key biophysical properties of AMPA receptors, which are implicated in learning and memory (Kessels and Malinow 2009). Most excitatory synaptic transmission in the brain being mediated through AMPAR, changes in the properties of these receptors are likely to have a major impact on brain function. Furthermore, GLUR2 was shown to bind directly to RSK2 in murine neurons suggesting a direct influence of RSK2 on GLUR2 function (Thomas et al. 2005). The GLUR family contains four closely related members (GLUR1-4). AMPARs are tetrameric, composed of various combinations of GLUR1-4 subunits, and the conductance properties of the receptors are highly dependent on their subunit composition (Kuner et al. 2001). GLUR2-lacking receptors have a higher Ca^{++} permeability, channel conductance, open probability and rectification than GLUR2-containing receptors (Isaac et al. 2007). Therefore, the presence or absence of the GLUR2 subunit can dramatically alter AMPAR properties and thereby synaptic transmission.

Our results provide evidence that in the hippocampus of *Rsk2*-KO mice total expression of GLUR2 is increased, and that the expression is also increased at the surface of synapses in cultured primary hippocampal cells. It was reported previously that surface insertion of GLUR2 occurs constitutively under basal conditions (Passafaro et al. 2001). Our results are compatible with these data. It may be speculated that over-representation of the GLUR2 subunit in synaptic AMPARs results in decreasing of Ca^{++} permeability and channel conductance. We show that there is, indeed, a 25% reduction in basal AMPAR-mediated transmission in the hippocampus of *Rsk2*-KO mice.

The Q/R site was completely edited in both WT and *Rsk2*-KO hippocampi, whereas the extent of R/G editing was significantly decreased. The GLUR2 subunit confers Ca^{++} impermeability on the channel due to a single arginine (R) residue located at amino acid position 607, which is a glutamine (Q) in the other AMPA receptor subunits. RNA editing of the Q/R site is specific to GLUR2 and is complete in postnatal brain. Our results in WT mice confirm further these latter data and show that Q/R editing is unaltered in *Rsk2*-KO mice. GLUR2-4 undergo also RNA editing [arginine (R) to glycine (G)] at amino acid position 743 (Lomeli et al. 1994). The presence of edited GLUR subunits at position 743 yields channels with faster kinetics. The R/G editing state of GLUR2–4 influences also the assembly and surface expression of AMPAR complexes. We show that R/G editing is significantly altered in *Rsk2*-KO mice. Finally, alternative splicing in the extracellular ligand binding domain of the AMPARs generates two variants, i.e., flip and flop. Native AMPAR are heteromeric assemblies of different subunits that may have different flip and flop isoforms. We show that in *Rsk2*-KO mice the proportion of GLUR2 molecules with a flop exon is significantly higher than in WT littermates. The flop variants desensitize at least 3 times faster but recover more slowly from desensitization than the flip counterparts (Pei et al. 2009). It was also previously shown that the flip/flop splicing has an effect on the maturation and cellular trafficking of AMPARs (Brorson et al. 2004). Alteration of R/G editing and splicing of GLUR2 in *Rsk2*-KO mice are therefore expected to alter AMPARs channel kinetic, desensitization and trafficking. Further functional studies are required to address the precise functional consequences of these editing and splicing changes in *Rsk2*-KO neurons. Furthermore, it was shown that proteins binding to GLUR2 are necessary for constitutive replacement of newly inserted GLUR1-containing receptors to maintain synaptic strength during LTP (Malinow and Malenka 2002). It has also been proposed that the expression of hippocampal LTD is critically dependent on GLUR2 (Malinow and Malenka 2002). Further studies will address the consequences of up-regulation of GLUR2 in *Rsk2*-KO mice for LTP and LTD. The signaling mechanisms involved in the increased levels of transcription of *Gria2* in *Rsk2*-KO hippocampal neurons are not yet known. The regulation of *Gria2* splicing and editing events is poorly understood as well. *Gria2* expression is influenced strongly at the transcriptional level by at least three regulatory elements in the 5′ proximal region of the promoter (Borges and Dingledine 2001). RNA editing is mediated by adenosine deaminase acting on RNA (ADAR) enzymes. Three structurally related ADARs (ADAR1 to ADAR3) have been identified in mammals. ADAR2 predominantly catalyzes RNA editing at the Q/R site of GLUR2 (Peng et al. 2006), whereas it is not yet clear how the R/G site is edited. The underlying mechanism of the R/G editing dysregulation may be caused by altered function or expression of one or several ADAR enzymes. However, the fact that editing of the Q/R site in GLUR2 is not affected in *Rsk2*-KO mice suggesting that ADAR2 is excluded. Further investigations are necessary to determine precisely the molecular events leading to up-regulation of the *Gria2* gene and alteration of RNA editing, and the contribution of each of these dysregulations to the cognitive dysfunction. The contribution of other pathways remains also to be investigated. Among the deregulated genes at least one other participates in regulation of AMPAR function: *Cacng8*. This gene encodes a synaptic protein, TARPγ-8 that participates in consolidation phase of memory and is involved in modulating neurotransmitter release. Evidence was provided that TARPγ-8 is critical for basal AMPAR expression and localization at extrasynaptic sites in the hippocampus (Rouach et al. 2005). Up-regulation of *Cacng8* may thus contribute to AMPAR dysfunction.

The data in this study provide a first glimpse of the gene expression profile of adult hippocampi in the absence of RSK2 expression. However, the *Rsk2*-KO animals represent a value model to study human Coffin–Lowry syndrome, it has significant limitations due to potential compensatory adaptation mechanisms in the developing nervous system (in particular through other RSK family members). Thus, it would be interesting to perform expression profiling following *Rsk2* gene silencing by RNA interference technology. Indeed, cellular or animal models based on this technology could offer further clues about the function of RSK2.

In conclusion, functional impairment of neurotransmission and plasticity due to AMPAR dysfunction may, indeed, contribute to the cognitive deficit of *Rsk2*-KO mice. However, further investigations are necessary to determine precisely the molecular events leading to alteration of GLUR2 expression and the contribution of this dysregulation to the cognitive dysfunction. The involvement of other pathways, including in particular cellular proliferation and apoptosis, remains also to be investigated.

Finally, the genes identified by our microarray analysis will help in further unravel the various functions of RSK2 in the hippocampus can be speculated to play a role in the pathogenesis of mental retardation in Coffin–Lowry syndrome and may provide targets for pharmaceutical intervention.

Accession number

The data of the expression arrays produced for this report have been submitted to NCBIs Gene Expression Omnibus (GEO: http://www.ncbi.nlm.nih.gov/geo/) and are accessible through GEO Series accession number GSE22137.

Acknowledgments The authors wish to thank Jessica Heringer for technical assistance and helpful discussions, and the IGBMC, Institut de Génétique et de Biologie Moléculaire et Cellulaire for assistance. This work was supported by the French National Agency for Research (Grant number 08-MNPS-021-01, to A.H.), the Fondation Jérôme Lejeune (to A.H.), the Centre National de la Recherche Scientifique, the Institut National de la Santé et de la Recherche, the College de France and the University of Strasbourg. AS was supported by a fellowship from the Ministere pour la Recherche et Technologie of France and TM by a scholarship from the Higher Education Commission (HEC) of Pakistan.

Conflict of interest The authors declare that they have no conflict of interest.

References

Benjamini Y, Hochberg Y (1995) Controlling the false discovery rate: a practical and powerful approach to multiple testing. J R Stat Soc B 57:289–300

Birnbaumer L, Qin N, Olcese R, Tareilus E, Platano D, Costantin J, Stefani E (1998) Structures and functions of calcium channel beta subunits. J Bioenerg Biomembr 30:357–375

Borges K, Dingledine R (2001) Functional organization of the GluR1 glutamate receptor promoter. J Biol Chem 276:25929–25938

Brand K, Page S, Walli AK, Neumeier D, Baeuerle PA (1997) Role of nuclear factor-kappa B in atherogenesis. Exp Physiol 82:297–304

Brorson JR, Li D, Suzuki T (2004) Selective expression of heteromeric AMPA receptors driven by flip-flop differences. J Neurosci 24:3461–3470

Carlson NG, Howard J, Gahring LC, Rogers SW (2000) RNA editing (Q/R site) and flop/flip splicing of AMPA receptor transcripts in young and old brains. Neurobiol Aging 21:599–606

Cheng CM, Mervis RF, Niu SL, Salem N Jr, Witters LA, Tseng V, Reinhardt R, Bondy CA (2003) Insulin-like growth factor 1 is essential for normal dendritic growth. J Neurosci Res 73:1–9

Davis S, Laroche S (2006) Mitogen-activated protein kinase/extracellular regulated kinase signalling and memory stabilization: a review. Genes Brain Behav 5(Suppl 2):61–72

De Cesare D, Jacquot S, Hanauer A, Sassone-Corsi P (1998) Rsk-2 activity is necessary for epidermal growth factor-induced phosphorylation of CREB protein and transcription of c-fos gene. Proc Nat Acad Sci USA 95:12202–12207

Frödin M, Gammeltoft S (1999) Role and regulation of 90 kDa ribosomal S6 kinase (RSK) in signal transduction. Mol Cell Endocrinol 51:65–77

Fu AK, Cheung WM (1999) Identification of genes induced by neuregulin in cultured myotubes. Mol Cell Neurosci 14:241–253

Ghate A, Befort K, Becker JA, Filliol D, Bole-Feysot C, Demebele D, Jost B, Koch M, Kieffer BL (2007) Identification of novel striatal genes by expression profiling in adult mouse brain. Neuroscience 146:1182–1192

Guimiot F, Delezoide AL, Hanauer A, Simonneau M (2004) Expression of the RSK2 gene during early human development. Gene Expr Patterns 4:111–114

Hanauer A, Young ID (2002) Coffin–Lowry syndrome: clinical and molecular features. J Med Genet 39:705–713

Isaac JT, Ashby M, McBain CJ (2007) The role of the GluR2 subunit in AMPA receptor function and synaptic plasticity. Neuron 54:859–871

Kessels HW, Malinow R (2009) Synaptic AMPA receptor plasticity and behavior. Neuron 61:340–350

Kim MD, Jan LY, Jan YN (2006) The bHLH-PAS protein Spineless is necessary for the diversification of dendrite morphology of *Drosophila* dendritic arborization neurons. Genes Dev 20:2773–2778

Kuner T, Beck C, Sakmann B, Seeburg PH (2001) Channel-lining residues of the AMPA receptor M2 segment: structural environment of the Q/R site and identification of the selectivity filter. J Neurosci 21:4162–4172

Lai F, Chen CX, Carter KC, Nishikura K (1997) Editing of glutamate receptor B subunit ion channel RNAs by four alternatively spliced DRADA2 double-stranded RNA adenosine deaminases. Mol Cell Biol 17:2413–2424

Lee JC, Greig A, Ravindranathan A, Parks TN, Rao MS (1998) Molecular analysis of AMPA-specific receptors: subunit composition, editing, and calcium influx determination in small amounts of tissue. Brain Res Protoc 3:142–154

Lomeli H, Mosbacher J, Melcher T, Höger T, Geiger JR, Kuner T, Monyer H, Higuchi M, Bach A, Seeburg PH (1994) Control of kinetic properties of AMPA receptor channels by nuclear RNA editing. Science 266:1709–1713

Lutz RE (2007) Trinucleotide repeat disorders. Semin Pediatr Neurol 14:26–33

Malinow R, Malenka RC (2002) AMPA receptor trafficking and synaptic plasticity. Annu Rev Neurosci 25:103–126

Marques Pereira P, Gruss M, Braun K, Foos N, Pannetier S, Hanauer A (2008) Dopaminergic system dysregulation in the mrsk2_KO mouse, an animal model of the Coffin–Lowry syndrome. J Neurochem 107:1325–1334

Nakamoto N, Nalavadi V, Epstein MP, Narayanan U, Bassell GJ, Warren ST (2007) Fragile X mental retardation protein deficiency leads to excessive mGluR5-dependent internalization of AMPA receptors. Proc Nat Acad Sci USA 39:15537–15542

Nishino I, Fu J, Tanji K, Yamada T, Shimojo S, Koori T, Mora M, Riggs JE, Oh SJ, Koga Y et al (2000) Primary LAMP-2 deficiency causes X-linked vacuolar cardiomyopathy and myopathy (Danon disease). Nature 406:906–910

Passafaro M, Piëch V, Sheng M (2001) Subunit-specific temporal and spatial patterns of AMPA receptor exocytosis in hippocampal neurons. Nat Neurosci 4:917–926

Pei W, Huang Z, Wang C, Han Y, Park JS, Niu L (2009) Flip and flop: a molecular determinant for AMPA receptor channel opening. Biochemistry 48:3767–3777

Peng PL, Zhong X, Tu W, Soundarapandian MM, Molner P, Zhu D, Lau L, Liu S, Liu F, Lu Y (2006) ADAR2-dependent RNA editing of AMPA receptor subunit GluR2 determines vulnerability of neurons in forebrain ischemia. Neuron 49:719–733

Poirier R, Jacquot S, Vaillend C, Soutthiphong AA, Libbey M, Davis S, Laroche S, Hanauer A, Welzl H, Lipp HP, Wolfer DP (2007) Deletion of the Coffin–Lowry syndrome gene Rsk2 in mice is associated with impaired spatial learning and reduced control of exploratory behavior. Behav Genet 37:31–50

Qin H, Powell-Coffman JA (2004) The *Caenorhabditis elegans* aryl hydrocarbon receptor, AHR-1, regulates neuronal development. Dev Biol 270:64–75

Rouach N, Byrd K, Petralia RS, Elias GM, Adesnik H, Tomita S, Karimzadegan S, Kealey C, Bredt DS, Nicoll RA (2005) TARP gamma-8 controls hippocampal AMPA receptor number, distribution and synaptic plasticity. Nat Neurosci 8:1525–1533

Sassone-Corsi P, Mizzen CA, Cheung P, Crosio C, Monaco L, Jacquot S, Hanauer A, Allis CD (1999) Requirement of Rsk-2 for epidermal growth factor-activated phosphorylation of histone H3. Science 285:886–891

Seidenman KJ, Steinberg JP, Huganir R, Malinow R (2003) Glutamate receptor subunit 2 serine 880 phosphorylation modulates synaptic transmission and mediates plasticity in CA1 pyramidal cells. J Neurosci 23:9220–9228

Thomas GM, Rumbaugh GR, Harrar DB, Huganir RL (2005) Ribosomal S6 kinase 2 interacts with and phosphorylates PDZ domain-containing proteins and regulates AMPA receptor transmission. Proc Nat Acad Sci USA 102:15006–15011

Wang Y, Tang BL (2006) SNAREs in neurons—beyond synaptic vesicle exocytosis. Mol Membr Biol 23:377–384

Xu D, Hopf C, Reddy R, Cho RW, Guo L, Lanahan A, Petralia RS, Wenthold RJ, O'Brien RJ, Worley P (2003) Narp and NP1 form heterocomplexes that function in developmental and activity-dependent synaptic plasticity. Neuron 39:513–528

Zeniou M, Ding T, Trivier E, Hanauer A (2002) Expression analysis of RSK gene family members: the RSK2 gene, mutated in Coffin–Lowry syndrome, is prominently expressed in brain structures essential for cognitive function and learning. Hum Mol Genet 11:2929–2940

Zou Y, Liu Q, Chen B, Zhang X, Guo C, Zhou H, Li J, Gao G, Guo Y, Yan C et al (2007) Mutation in CUL4B, which encodes a member of cullin-RING ubiquitin ligase complex, causes X-linked mental retardation. Am J Hum Genet 80:561–566